



## OPEN

SUBJECT AREAS:  
CANCER GENOMICS  
LEUKAEMIA  
HAEMATOLOGICAL CANCERReceived  
11 June 2014Accepted  
15 September 2014Published  
9 October 2014Correspondence and  
requests for materials  
should be addressed to  
S.K.B. (s.bohlander@  
auckland.ac.nz)Identification and characterization of  
*OSTL (RNF217)* encoding a  
RING-IBR-RING protein adjacent to a  
translocation breakpoint involving *ETV6*  
in childhood ALLLuciana M. Fontanari Krause<sup>1</sup>, Anna Sophia Japp<sup>1</sup>, Alexandre Krause<sup>1</sup>, Jana Mooster<sup>2</sup>, Martin Chopra<sup>3</sup>,  
Markus Müschen<sup>4</sup> & Stefan K. Bohlander<sup>1,3</sup><sup>1</sup>Department of Internal Medicine III, University Hospital Grosshadern, Ludwig Maximilians-Universität, Munich (LMU), Germany, <sup>2</sup>Laboratory for Molecular Stem Cell Biology, Institute for Transplantation Diagnostics and Cell Therapeutics, Heinrich-Heine-Universität, Düsseldorf, Germany, <sup>3</sup>Faculty of Medical and Health Sciences, Department of Molecular Medicine and Pathology, The University of Auckland, Auckland, New Zealand, <sup>4</sup>Department of Laboratory Medicine, University of California San Francisco, San Francisco, California, USA.

Genomic aberrations involving *ETV6* on band 12p13 are amongst the most common chromosomal abnormalities in human leukemia. The translocation t(6;12)(q23;13) in a childhood B-cell acute lymphoblastic leukemia (ALL) cell line fuses *ETV6* with the putative long non-coding RNA gene *STL*. Linking *STL* properties to leukemia has so far been difficult. Here, we describe a novel gene, *OSTL* (annotated as *RNF217* in Genbank), which shares the first exon and a CpG island with *STL* but is transcribed in the opposite direction. Human *RNF217* codes for a highly conserved RING finger protein and is mainly expressed in testis and skeletal muscle with different splice variants. *RNF217* shows regulated splicing in B cell development, and is expressed in a number of human B cell leukemia cell lines, primary human chronic myeloid leukemia, acute myeloid leukemia with normal karyotype and acute T-ALL samples. Using a yeast two-hybrid screen, we identified the anti-apoptotic protein HAX1 to interact with *RNF217*. This interaction could be mapped to the C-terminal RING finger motif of *RNF217*. We propose that some of the recurring aberrations involving 6q might deregulate the expression of *RNF217* and result in imbalanced apoptosis signalling via HAX1, promoting leukemia development.

Recurrent chromosomal translocations are commonly found in human leukemia and constitute the molecular basis for many hematopoietic malignancies<sup>1–3</sup>. Leukemic transformation by such aberrations is mainly driven by either the formation of fusion proteins with novel characteristics or by the deregulation of oncogene expression<sup>4–6</sup>. Genomic aberrations involving the gene *E-Twenty-Six (ETS) Variant 6 (ETV6)* gene on band 12p13 are amongst the most common chromosomal abnormalities observed in human leukemia. The *ETS* domain transcription factor *ETV6* can be fused to more than 30 different partners, including protein tyrosine kinases as *PDGFRB*, *ABL1* and 2, and *JAK2*, and a number of transcription factors including *RUNX1*<sup>7–9</sup>.

In 1997, we identified a novel fusion partner of *ETV6*, which we named *Six-Twelve-Leukemia (STL)* gene<sup>10</sup>. *STL* was cloned from the childhood B-cell ALL cell line SUP-B2 (ref. 11) that has a t(6;12)(q23;p13) translocation and a deletion of the 12p13 region of the normal chromosome 12 and therefore lacks wildtype *ETV6* (ref. 12). The current annotation localizes *STL* to 6q22.31. Whereas 6;12 translocations by themselves are recurrent but quite rare<sup>12,13</sup>, 6q is a genomic region frequently deleted in lymphoblastic leukemia and lymphomas<sup>13–15</sup>. The *STL* sequence does not contain any long open reading frames, and if the reading frame of *ETV6* is continued into *STL* in the *ETV6/STL* fusion transcript, a stop codon is encountered after 14 amino acids<sup>10</sup>. It has been difficult to propose a mechanism by which the *ETV6/STL* fusion might drive leukemogenic transformation as no apparent function can be attributed to the *STL* gene.

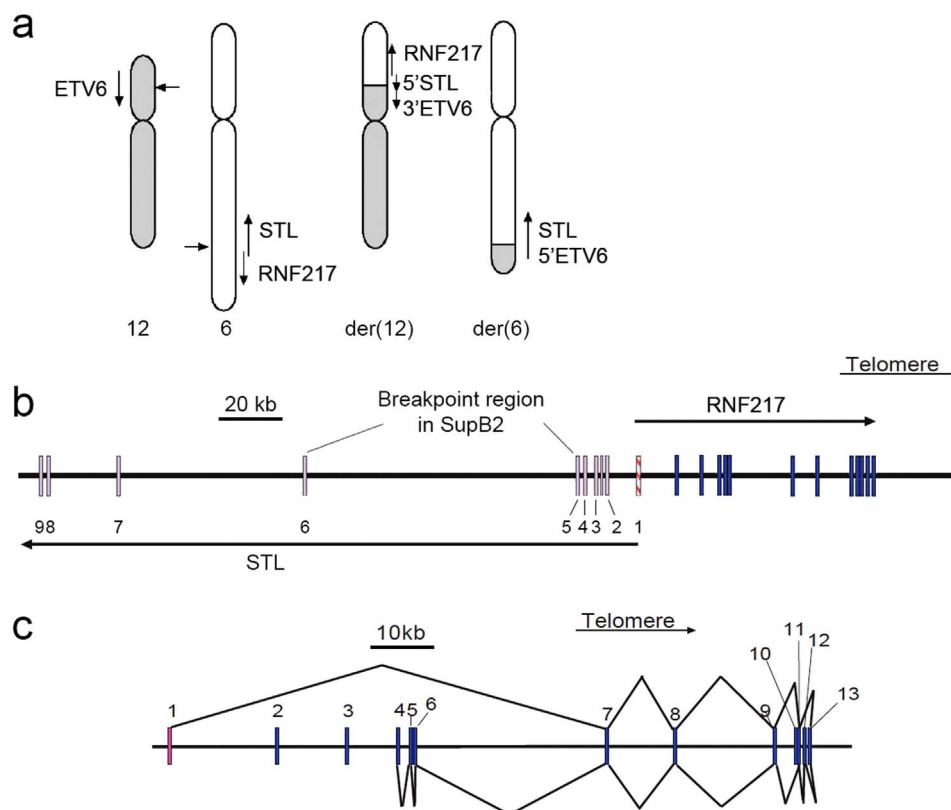


**Figure 1 | Genomic organization of the ETV6/STL fusion and the STL/RNF217 locus.** (a) The t(6;12)(q23;p13) genomic rearrangement. (b) *RNF217* shares the first exon with *STL* but is transcribed in the opposite direction. (c) Exon-intron organization of the *RNF217* gene with two possible splice variants.

Here, we describe a novel gene, *opposite STL* (*OSTL*), which shares the first exon and a CpG island with the putative long non-coding (nc)RNA gene *STL* but is transcribed in the opposite direction. *RNF217* codes for a 284 amino acid protein with two RING finger domains linked by an in-between-RING fingers (IBR) motif. The *RNF217* protein is highly conserved across species and is expressed in various tissues. *RNF217* expression can be detected in a number of human leukemia cell lines and it is overexpressed in myeloid leukemia patient samples. Using a yeast two-hybrid screen, we demonstrated the *RNF217* protein to interact with HAX1, a protein involved in apoptotic signaling. We propose that the leukemogenic properties of the ETV6/STL fusion may not arise from a fusion protein but rather from the disruption or the transcriptional deregulation of the *STL/RNF217* locus. The high expression of *RNF217* in certain human leukemias suggests that the deregulation of this gene could be a more common mechanism in leukemogenesis.

## Results

**Genomic organization of the STL/RNF217 locus.** We have previously identified the t(6;12)(q23;p13) ETV6/STL fusion (Figure 1a) as a potentially recurrent genomic rearrangement in human leukemia<sup>10</sup>. As *STL* itself has no apparent open reading frame and in the ETV6/STL fusion transcript the *STL* portion only extends the ETV6 open reading frame by 14 amino acids, we assessed the genomic locus around the *STL* gene in order to find genes near the breakpoint that might possibly be deregulated due to the genomic rearrangement. Doing so, we identified *Opposite of STL* (*OSTL*, also annotated as ring finger protein, *RNF217*, or in-between-RING finger domain-containing *IBRDC1*) sharing the first exon with *STL*, but being transcribed in the opposite direction (Figure 1b). The *STL* gene in Figure 1b (sequence in Supplementary Figure S1) is derived from our previous study<sup>10</sup> and differs from the UCSC

annotation (uc003pzq.3) in its centromeric, 3' portion. The human *STL/RNF217* genomic locus spans more than 450 kbp on 6q22.31. *STL* is also annotated as *RNF217-AS1* in the genenames.org database, indicating that *STL* could act as an antisense transcript for *RNF217*. Nevertheless, it has to be kept in mind that *STL* only overlaps with the first exon of *RNF217*. The *RNF217* gene is composed of 13 exons (Figure 1c, Supplementary Table S1). In the human *RNF217* cDNA sequence (Ensembl *RNF217-202*, Transcript ID ENST00000560949, Supplementary Figure S2), the second start codon (ATG, underlined) probably represents the true translational start site, because it is embedded in a better Kozak consensus sequence and it is homologous to the ATG in mouse *Rnf217* (Supplementary Figure S3). Both start codons are located within the first exon of the *RNF217* gene, which is associated with a CpG island. The *RNF217* transcript is subject to extensive alternative splicing. We identified at least 7 putative protein encoding splice variants of *RNF217* (Supplementary Table S2).

### **RNF217 is a highly conserved member of the RING finger family of proteins.**

The open reading frame of the human *RNF217* encodes a 284 amino acid protein (when using the second ATG as the start codon) with a calculated molecular mass of 30 kDa (Figure 2a). A database search against the *RNF217* protein sequence identified three domains, a variant N terminal RING finger (RING1), an IBR, also known as double RING finger linked motif (DRIL), and a consensus RING finger (RING2) at the C terminal end. Comparison between the consensus sequence and the *RNF217* RING motifs revealed the *RNF217* RING1 to have a lysine residue rather than a histidine residue at the H<sub>4</sub> position. The spacing between cysteines 7 and 8 in RING1 is 4 amino acids in *RNF217* compared to 2 amino acids in the consensus (Figure 2a). *RNF217* is highly conserved across species. Sequence comparison revealed 98.6% amino acid identity between human and mouse *RNF217*, 76.8% between

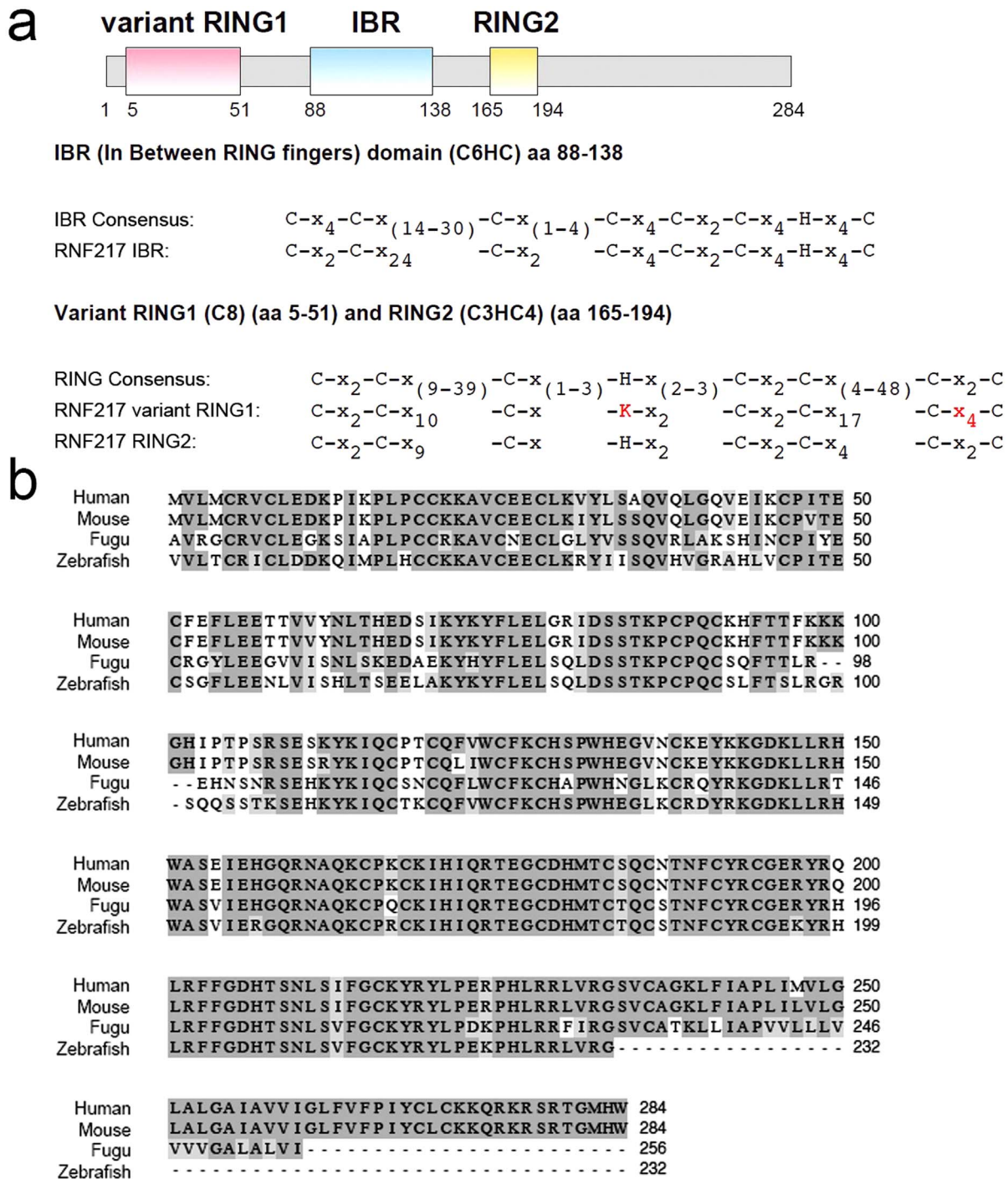


**Figure 2** | RNF217 is a highly conserved member of the RING finger family of proteins. (a) Diagram of the RNF217 protein with its functional domains annotated. Comparison of the RNF217 protein domains to the consensus sequences. (b) Protein sequence comparison of the human, mouse, Fugu, and zebrafish RNF217 proteins.

human and *Fugu rubripes* (puffer fish) Rnf217, and 79.6% between human and *Danio rerio* (zebrafish) Rnf217 (Figure 2b).

**Tissue-specific expression of RNF217.** We analyzed the expression of RNF217 in various human tissues using a human multiple tissue Northern blot (Figure 3a). RNF217 transcripts of 9.5 and 4.4 kbp were detected in a number of tissues. The strongest expression was detected in testis (with an additional transcript of 1.35 kbp) and in skeletal muscle (with an additional transcript of 2.4 kbp). Weaker expression was detected in prostate, ovary, heart, placenta, liver, and pancreas.

**Expression of RNF217 in human B cell leukemia cell lines and B cell developmental stages.** We hypothesized that the tissue-restricted expression of RNF217 might be deregulated in human B cell leukemia<sup>10,13-14</sup>. To test this, we analyzed the mRNA expression of this gene in a number of human leukemia cell lines by RT-PCR (Figure 3b). A 160 bp fragment was amplified in the mature B cell NHL cell line Granta 519 (ref. 16), two Epstein Barr virus transformed lymphoblastoid cell lines (LCL B and LCL D) and in the precursor B-cell ALL cell line SEM<sup>17</sup>. The expression of RNF217 does not correlate with reported deletions of 12p13 or the STL/RNF217 locus in these cell lines. Next, we assessed different B cell

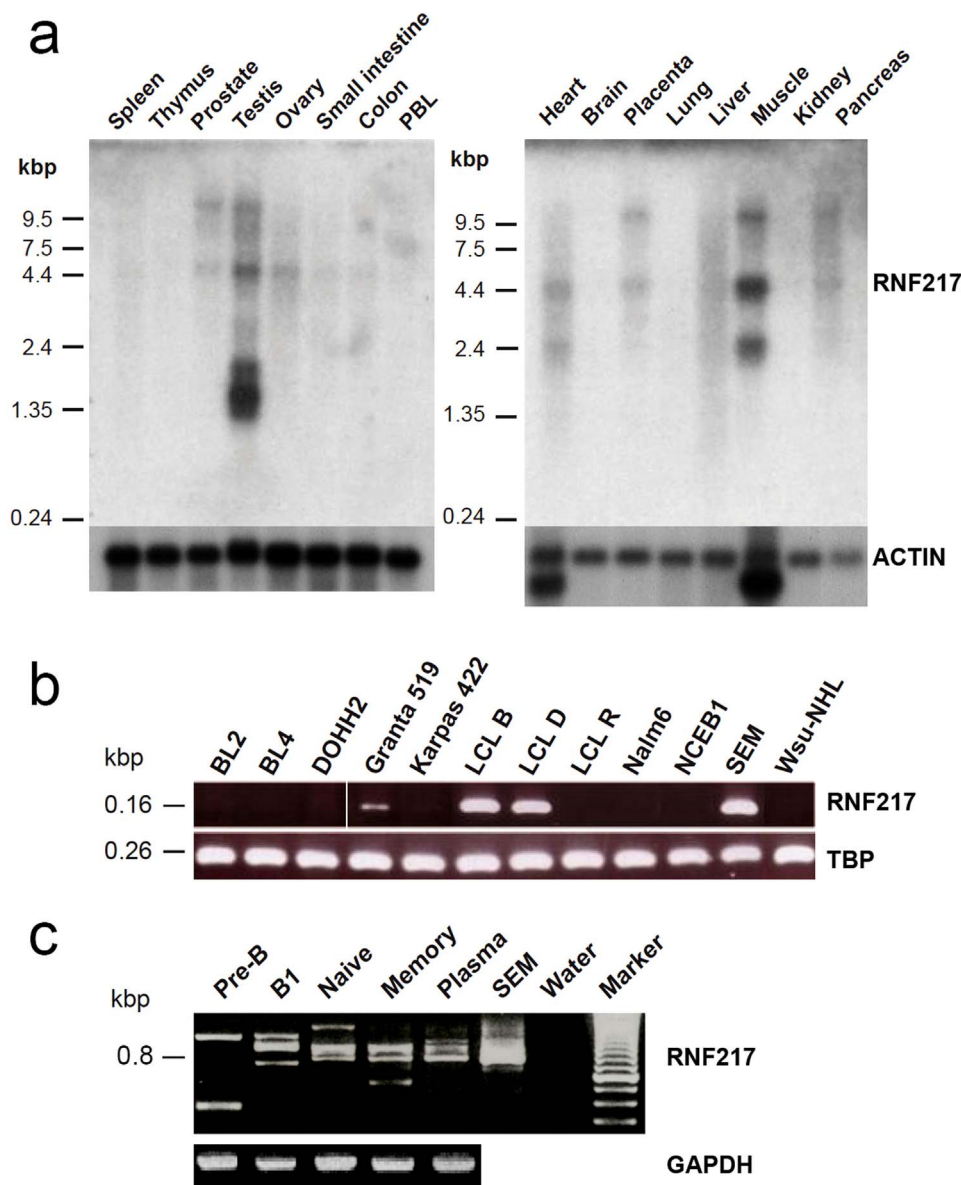


**Figure 3** | Expression of *RNF217* in human tissues and B cells. (a) Multiple human tissue northern blot hybridized with a radioactively labeled *RNF217* probe. (b) Cell lines derived from human B cell neoplasms were analyzed for their expression of *RNF217* by RT-PCR. *TBP* expression was assessed as a control. The primers that were used for this experiment covered exons 9 and 11 of the *RNF217* gene (see Supplementary table 1), to allow for the detection of all putative protein-coding splice variants shown in Supplementary table 2. Note that the *RNF217* gel picture is a composite of two different gels. (c) Determination of *RNF217* expression and splicing during B cell development. *GAPDH* expression was assayed as control.

developmental stages for their expression of *RNF217* (Figure 3c). Distinct transcripts of various sizes could be amplified from all developmental stages indicating tightly regulated alternative splicing of *RNF217* over the course of B cell development. The SEM cell line was used as a positive control for *RNF217* expression.

***RNF217* expression in primary bone marrow samples from human leukemia patients.** To further assess the potential contribution of *RNF217* to human leukemia, we analyzed primary bone marrow samples derived from leukemia patients (Figure 4a). *RNF217* was expressed in normal bone marrow and expression levels varied among both AML and ALL samples. We analyzed microarray data from 129 leukemia patient and 10 normal bone marrow samples to quantitatively assess *RNF217* expression levels across 12 different leukemia types in comparison to normal bone marrow cells. This screening revealed CML samples to have the highest relative expression levels of *RNF217* (Figure 4b). Quantitative RT-PCR

analysis of 19 ALL and 20 myeloid leukemia samples (10 CML and 10 AML samples with normal karyotype) proved myeloid leukemia samples to have an overall higher expression of *RNF217* compared to lymphoblastic leukemia samples (AML vs. ALL  $P=0.0096$ ; CML vs. ALL  $P=0.0006$ ) with the AML samples having slightly higher expression levels than the CML samples (Figure 4c).

**Identification of *RNF217* interacting proteins.** The *STL/RNF217* genomic locus at 6q22.31 is close to frequent targets of genomic aberrations<sup>12–15</sup> and *RNF217* is highly expressed in human myeloid leukemias when compared to normal bone marrow. We therefore assumed that the deregulation of *RNF217* might be a potential driver of human leukemogenesis and were interested in mechanisms of how *RNF217* might promote leukemia. To this end, we performed a yeast two-hybrid protein interaction screen to identify interaction partners of *RNF217*. The *RNF217* protein served as bait to screen a HeLa S3 cDNA prey library. Of 24 prey clones that were identified in the

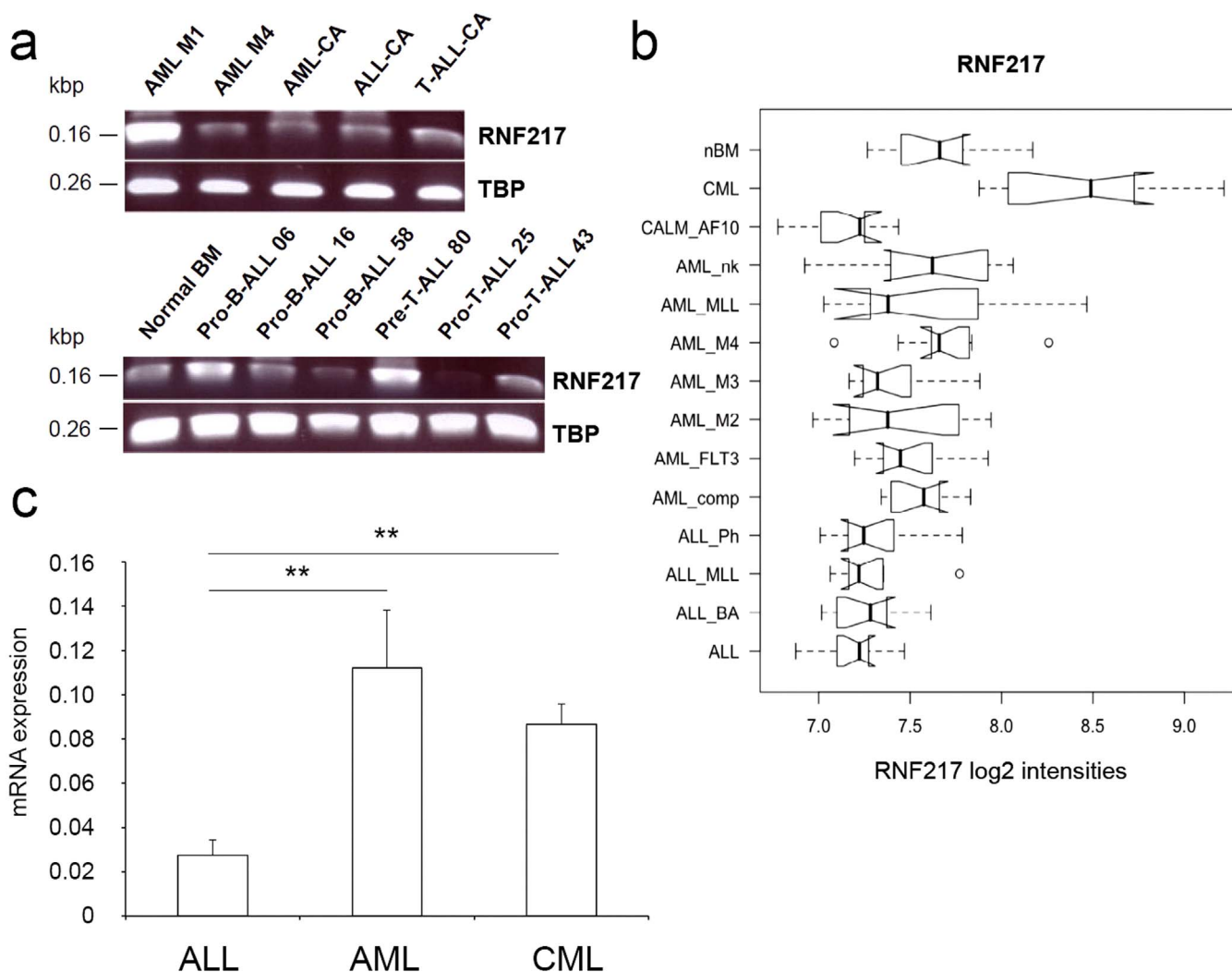


**Figure 4 | Expression of *RNF217* in primary human leukemia samples.** (a) Primary human bone marrow samples from leukemia patients were analyzed for their expression of *RNF217* by RT-PCR. *TBP* expression was assayed as a control. (b) Microarray expression profiles of primary human bone marrow samples from leukemia patients<sup>19</sup> were generated. Data for *RNF217* expression was log<sub>2</sub> transformed and evaluated (normal bone marrow (nBM; n=10), CML; n=10, *CALM/AF10*-positive AML (*CALM\_AF10*; n=10), AML with normal karyotype and FLT3 negative (*AML\_nk*; n=10), AML with MLL rearrangement (*AML\_MLL*; n=9), AML with *inv(16)(p13q22)* (*CBFβ-MYH11* fusion, *AML\_M4*; n=10), AML with *t(15;17)(q21;q22)* (*PML-RARA* fusion, *AML\_M3*; n=10), AML with *t(8;21)(q22;q22)* (*AML1-ETO* fusion, *AML\_M2*; n=10), AML with normal karyotype and FLT3-ITD (*AML\_FLT3*; n=10), AML with complex aberrant karyotype (*AML\_comp*; n=10), ALL with *t(9;22)(q34;q11)* (*BCR-ABL* fusion, *ALL\_Ph*; n=10), ALL with *t(4;11)(q21;q23)* rearrangement (*MLL-AF4* fusion, *ALL\_MLL*; n=10), common ALL (*ALL\_BA*; n=10), and pro-B ALL (*ALL*; n=10)). The probe set for *RNF217* on the microarrays used (Affymetrix HGU133, probe set 235492\_AT) detects exon 13 of human *RNF217* (see Supplementary table 1). This exon is part of all splice variants shown in Supplementary table 2. (c) *RNF217* expression in primary human bone marrow samples from leukemia patients was assessed by quantitative RT-PCR with *β-actin* as reference gene. Expression levels were calculated from  $c_T$  values by the  $2^{-\Delta c_T}$  method (*ALL*; n=19, *AML*; n=10, *CML*; n=10), Mean ± standard error of mean. \*\*  $P \leq 0.01$ . The primers used for this experiment span exons 11 and 12 of the human *RNF217* gene (see Supplementary table 1). It has to be noted that not all of the identified putatively protein-coding splice variants of *RNF217* contain exon 12 (see Supplementary table 2), therefore it is possible that not all splice variants of this gene in the leukemic samples might have been detected.

screen, 8 contained either the full-length open reading frame of HS1-associated protein X-1 (HAX1) or parts of it (Figure 5).

**Mapping of the *RNF217* interaction domain with HAX1.** To define which region of the *RNF217* protein mediates the interaction with HAX1, several deletion mutants were constructed and assayed by using the two-hybrid system (Figure 6a and b). Colonies could only grow if the RING1 domain of *RNF217* was present, demonstrating the necessity for this domain in the protein-protein interaction with HAX1. The physical interaction between *RNF217* and HAX1 was further confirmed by co-immunoprecipitation of *in vitro* translated myc- and HA-tagged *RNF217* and HAX1 proteins, respectively, (Figure 6c) and after co-

transfecting CFP-*RNF217* and YFP-HAX1 into HEK293T cells (Figure 6d). Finally, immunofluorescence microscopy of NIH3T3 mouse fibroblast cells co-transfected with CFP-*RNF217* and YFP-HAX1 revealed cytoplasmic co-localization of the two proteins (Figure 6e).

## Discussion

Chromosomal rearrangements, especially balanced chromosomal translocations are common events in human leukemia. Many fusion proteins and gene deregulations resulting from these translocations are active drivers of leukemogenesis with known transformational mechanisms<sup>1-5,18-21</sup>. Apart from obviously functional fusions, it is of utter clinical importance to understand the leukemogenic mechan-

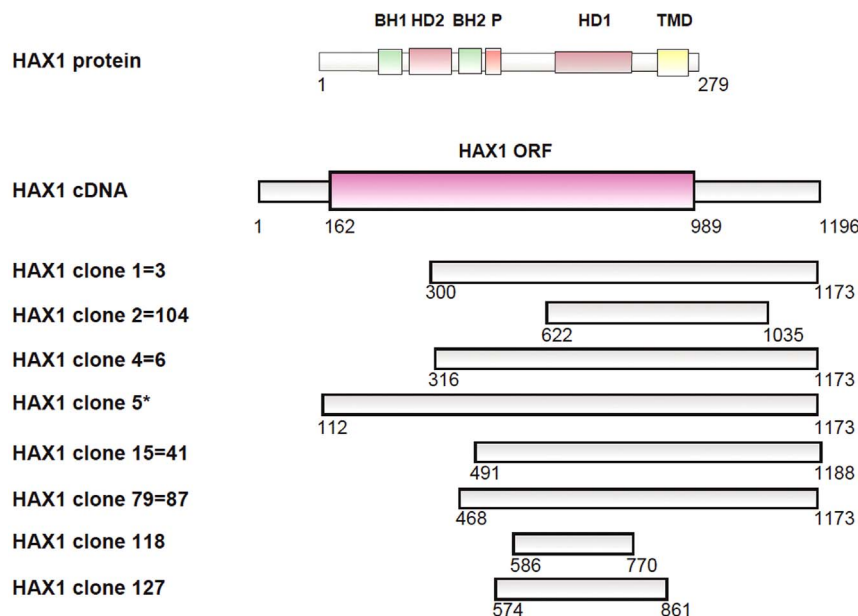


**Figure 5 | Result from the yeast two-hybrid screen.** AH109 yeast cells were co-transformed with pGAD-GH prey plasmids containing the human cDNA HeLa S3 library and the pGBKT7-RNF217 bait plasmid. Positive clones were sequenced. Of 24 positive clones, 8 contained either the full-length open reading frame of HS1-associated protein X-1 (HAX1), or parts of it as shown. \* HAX-1 clone 5 was used in the yeast two-hybrid experiments to confirm interaction with RNF217.

isms of recurrent genomic rearrangements that do not result in apparent fusion proteins or in the obvious transcriptional regulation of breakpoint adjacent genes.

We previously described a fusion between *ETV6* on chromosome 12 band p13, and *STL* on 6q23 (ref. 10). The functional consequences of the *ETV6/STL* fusion transcript are difficult to interpret as *STL* does not contain an obvious open-reading frame, and the *STL* portion in the *ETV6/STL* fusion only adds a short 14 amino acid tail to the first 54 amino acids of the *ETV6* protein<sup>10</sup>. An alternative explanation for recurrent 6;12 translocations<sup>12,13</sup> and frequent deletions on 6q<sup>13–15</sup> could be the deregulation of a gene close to the breakpoints of these rearrangements.

We analyzed the *STL* genomic locus and identified a novel gene, *OSTL* (probable E3 ubiquitin protein ligase *RNF217*), which shares the first exon and a CpG island with the putative long ncRNA *STL* but is transcribed from the opposite DNA strand in the opposite direction. The protein encoded by *RNF217* is highly conserved in evolution in vertebrates and harbors important protein domains (RING domains), putatively involved in the ubiquitination of proteins<sup>22</sup>. Deregulated ubiquitination has wide implications in human leukemia<sup>23–26</sup> and the successful introduction of proteasome inhibitors for the treatment of multiple myeloma proved that the ubiquitin-proteasome system is a valid therapeutic target in leukemia including AML<sup>27–29</sup>.

We demonstrated *RNF217* to be expressed mainly in testes and skeletal muscle. Interestingly, the expression pattern of *RNF217* resembles that of *STL*<sup>10</sup>, indicating co-regulation of the two genes. This assumption is further strengthened by the fact that exon 1, which is shared by *STL* and *RNF217*, is associated with the only CpG island found in the entire *STL/RNF217* locus, which spans close to 450 kbp (chr6:124,976,000–125,414,000, hg19). Tagawa and colleagues described genomic rearrangements at 6q21–22 in two T-cell lymphoma cell lines, which affected the gene adjacent to the *RNF217* gene towards the centromer (*NKAIN2*, *TCBA1*). One of the breakpoints described by Tagawa and colleagues was within the *STL* locus, supporting a possible involvement of the *STL/RNF217* locus in lymphomagenesis<sup>30</sup>.

Human B cell leukemia cell lines and primary bone marrow samples from leukemic patients expressed *RNF217* to varying levels.

Quantitative expression analysis by both RT-PCR and microarrays revealed patients with chronic myeloid leukemia and acute myeloid leukemia with a normal karyotype to have the highest levels of *RNF217* expression among our cohort. Even though the *ETV6/STL* fusion was initially cloned from a B cell acute lymphoblastic leukemia cell line, the expression levels of *RNF217* were highest in myeloid leukemia patient samples in our study. Publicly available data shows varying expression of *RNF217* in the human hematopoietic compartment and in hematopoietic malignancies with myeloid leukemia showing considerably higher expression of *RNF217* than lymphoid leukemias (ist.mediasapiens.com, Supplementary Figure S4). Although *RNF217* is not recurrently mutated in hematologic malignancies (0.18% mutation frequency), it is a frequent target for copy number alterations in solid tumors as summarized in the Catalogue of somatic mutations in cancer (COSMIC) database.

Gorbea and colleagues identified *RNF217* as an interaction partner of the 26 S proteasome-binding protein *ECM26* using a genome-wide two hybrid screen and mass spectrometry<sup>31</sup>. No other protein-interactions of *RNF217* have been described so far. Performing a yeast two-hybrid screen and co-immunoprecipitation experiments, we identified the anti-apoptotic protein *HAX1* to interact with *RNF217*. This interaction is mediated by the RING1 domain of *RNF217* that is encoded by both exons 1 and 7 (Supplementary Table S2 and Supplementary Figure S2). It has to be noted that not all of the splice variants that we could identify in this study contain exon 7 and therefore it seems plausible that not all *RNF217* proteins are able to interact with *HAX1*.

*HAX1* was initially found as an interaction partner of *HS1*, an intracellular protein that mediates signaling triggered by antigen receptor activation. The 35 kDa *HAX1* protein is ubiquitously expressed<sup>32</sup> (see also ist.mediasapiens.com, Supplementary Figure S5) and localizes mainly to mitochondria<sup>32</sup>. It plays an essential role in the maintenance of the mitochondrial membrane potential – and thereby prevents the initiation of the cell intrinsic, mitochondria-mediated apoptosis pathway<sup>33</sup>. *HAX1* contains two Bcl-2 homology domains, which indicates its anti-apoptotic function to be related to BH domain oligomerization. It further harbors a PEST sequence, and a putative transmembrane domain. The PEST sequence is responsible for *HAX-1* being conjugated with K48-linked ubiquitin chains

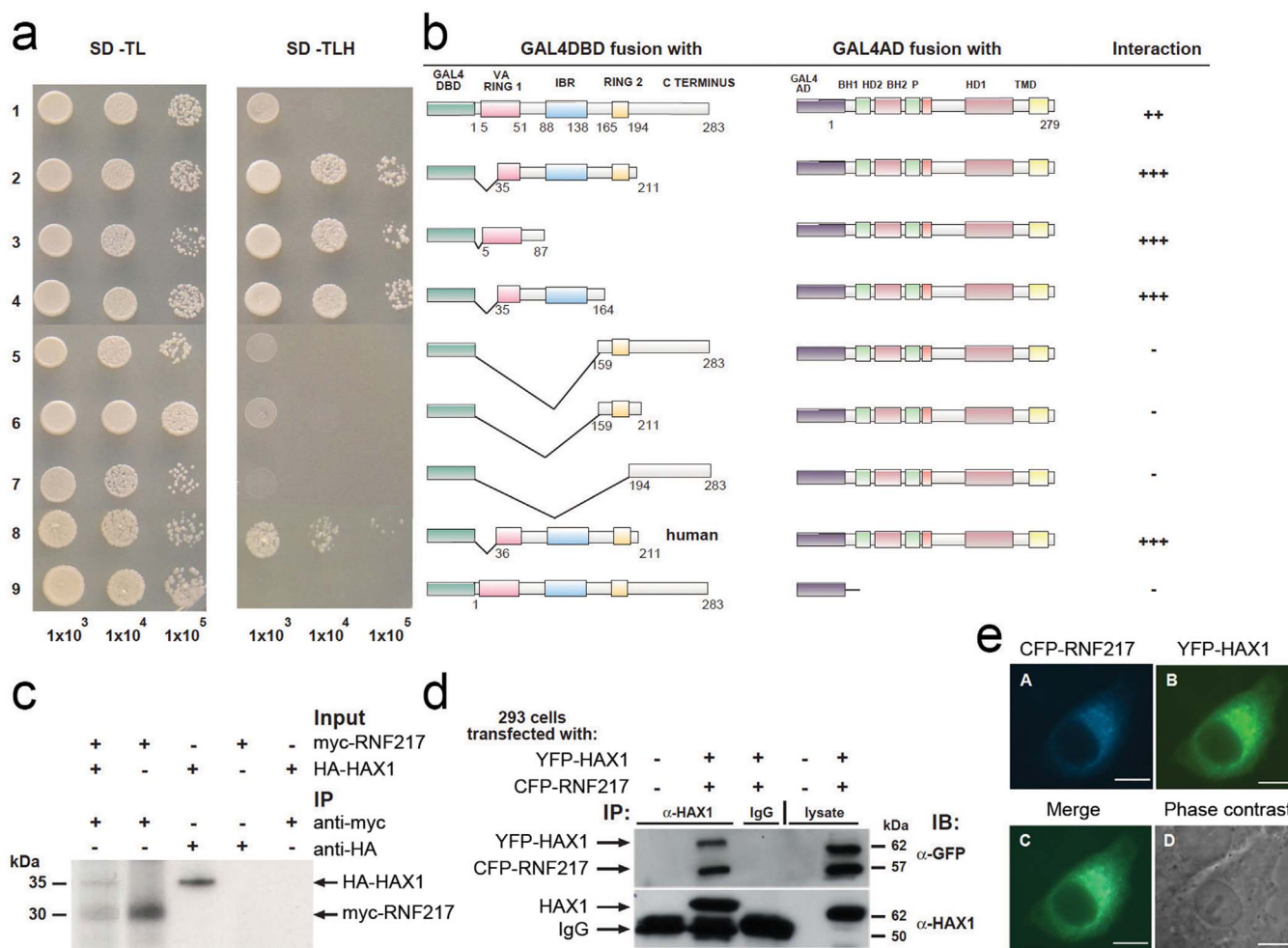


**Figure 6 | Confirmation and mapping of the RNF217-HAX1 interaction.** (a) and (b) The pGBKT7 plasmid containing RNF217 deletion mutants and the pGADT7 plasmid containing full-length HAX1 were co-transformed into AH109 yeast cells to map the interaction domains of RNF217. (c) *In vitro* translated [<sup>35</sup>S]-HA-RNF217 and -myc-HAX1 were mixed 1 : 1 and immunoprecipitated with an anti-myc antibody. Proteins were separated by SDS-PAGE and the gel was subjected to autoradiography. (d) pCFP-RNF217 and pYFP-HAX1 were co-transfected into HEK293T cells and the cells were lysed 24 h later. HAX1 was immunoprecipitated and proteins were separated by SDS-PAGE and CFP-RNF217 was detected using a mouse anti-GFP antibody. (e) NIH3T3 cells were transiently transfected and grown on cover slips for 12-24 h after transfection. Cells were fixed, mounted on glass slides, and analyzed using an inverted fluorescence microscope.

and degraded, demonstrating the interplay between polyubiquitination and apoptosis-inhibition by HAX1 (ref. 34). HAX1 interacts with several integral parts of the intracellular apoptosis machinery and can be cleaved by various pro-apoptotic proteases<sup>35-37</sup>. HAX1 promotes Omi/HrtA2 processing and thereby attenuate apoptosis<sup>38</sup>, it prevents the polyubiquitination and subsequent proteasomal degradation of the anti-apoptotic protein XIAP<sup>39</sup>, and inhibits caspase 9 activation<sup>40</sup>. Ectopic expression of HAX1 promotes esophageal squamous carcinoma cell proliferation and chemoresistance *in vitro* and increases tumor growth *in vivo* in a xenograft mouse model, whereas knock-down of HAX1 has opposite effects<sup>41</sup>.

HAX1 is highly expressed in human malignancies of mature B cells (CLL, myeloma, plasma cell leukemia), whereas its expression is lower in CML and AML<sup>42</sup> (see also [ist.medisapiens.com](http://ist.medisapiens.com), Supplementary Figure 5). Interestingly, HAX1 may replace BCL-2 when it comes to the necessity for the expression of anti-apoptotic proteins in lymphomas<sup>42</sup>. The preferred overexpression in B cell leukemias might mirror the dependency of normal B cell development on HAX1. Indeed, a study employing HAX1 deficient mice demonstrated severe B cell developmental defects<sup>43</sup>.

Klein and colleagues found HAX1 deficiency to be the cause for Kostmann disease, an autosomal recessive primary immunodeficiency

syndrome with severe congenital neutropenia (OMIM 610738)<sup>33</sup>. This disorder is characterized by increased neutrophil apoptosis and demonstrates HAX1 to be an important player in myeloid homeostasis. The molecular mechanism appears to be a defect in G-CSF-triggered granulopoiesis<sup>44</sup>. Of particular interest is the fact that patients suffering from Kostmann disease are prone to myelodysplastic syndrome and AML<sup>45</sup>.

The fact that one third of the RNF217 interacting prey clones identified in our yeast two hybrid screen contained HAX1 sequences suggest that HAX1 is a very prominent interaction partner of RNF217. Considering the important role of HAX1 in apoptosis homeostasis and its involvement in the development and malignant diseases of both the B lymphoid and myeloid lineage argue for an important role of RNF217 in this context as well. Loss of the *STL/RNF217* locus and subsequent deregulation of HAX1 degradation might result in shifting apoptotic balance towards cell survival, contributing to malignant transformation and leukemia progression.

The *STL/RNF217* locus shows a peculiar organization of an ncRNA gene (*STL*) and a very conserved protein-coding gene (*RNF217*) sharing a common first exon and a CpG island. Genomic loci with a similar organization are frequently imprinted or show allelic exclusion<sup>46-48</sup>. *STL* might be a *cis*-acting antisense



transcript or alternatively regulate *RNF217* by transcriptional interference. This is emphasized by the alternative annotation of *STL* as *RNF217-AS1* (genenames.org). Nevertheless, it has to be kept in mind that *STL* only overlaps with the first exon of *RNF217*. Examples for overlapping *cis*-acting ncRNAs include the *Xist/Tsix* locus that is essential in X chromosome inactivation<sup>49</sup>, the *Kcnq1* locus<sup>50</sup>, and the *IGF2R/AIRN* locus<sup>51,52</sup>. Loci in which both an ncRNA and an adjacent gene share their respective first exons and a common GpC island include e.g. the *IGF2* gene and its antisense ncRNA involved in Beckwith-Wiedemann and Russell-Silver syndromes<sup>53</sup>, and Wilm's tumor<sup>54</sup>, the *LEF1* gene, which is important in T cell development<sup>55</sup>, and the *HOXA6/HOXA-AS3* transcript variant 1 locus.

Considering the unusual structure of the *STL/RNF217* locus and the lack of an obvious *ETV6/STL* fusion protein, a possible mechanism for the leukemogenic effect of the t(6;12)(q23;p12) translocation could be a transcriptional deregulation of the *RNF217* gene. There are at least two mechanisms that could lead to *RNF217* deregulation: 1) disruption of the *STL* gene and subsequent loss of its putative *cis*-acting influence on *RNF217*; 2) an intronic enhancer from the *ETV6* locus might lead to increased expression of *RNF217*, a mechanism that has been proposed for several other *ETV6* rearrangements<sup>9,56–59</sup>.

Deregulated *RNF217* expression might cause apoptotic imbalance due to interference with HAX1 degradation. The strong phenotype associated with genetic disorders involving HAX1 supports an important role for HAX1 in human hematopoiesis and leukemogenesis<sup>33,41–45</sup>. On the one hand, *RNF217* is highly expressed in some human leukemias, on the other hand, the *STL/RNF217* locus is a frequent target of gene loss in human B cell neoplasias<sup>10,13–15</sup>. This all suggests that the deregulation of this protein should be further explored as a possible mechanism of leukemogenesis. However, it needs to be noted that to formally prove a link between *RNF217* and leukemia, animal models overexpressing *RNF217* need to be developed and the molecular functions of *RNF217* need to be studied.

## Methods

**Patient samples.** Bone marrow samples were collected from leukemic patients. Peripheral blood and bone marrow samples for B cell sorting were collected from healthy donors. Informed consent was obtained in accordance with the declaration of Helsinki and local ethical guidelines. *RNF217* expression was analyzed in a microarray dataset published by us in 2012 (ref. 19). For the RT-PCR experiments, patient samples were obtained from diagnostic leukemia samples acquired from 2000 to 2009 (Laboratory for Leukemia Diagnostics, Department of Medicine III, Grosshadern, Ludwig Maximilians University, Munich, Germany). The study was approved by the institutional review board (Ludwig-Maximilians-University [LMU]-Munich).

**Cell lines.** BL2, BL4, DOHH2, Granta 519, Karpas 422, NCEB1, and Wsu-NHL cell lines were provided by Martin Dreyling, Department of Medicine III, Munich, Germany. LCL B, LCL D, and LCL R cell lines were provided by Martin Schlee, and the SEM cell line by Georg Bornkamm, both Helmholtz Zentrum Munich, Munich, Germany.

**Plasmid construction.** The bait plasmids for the yeast two-hybrid screen were generated by inserting either the full length *RNF217* cDNA or different *RNF217* deletion mutants (1. Full-length *RNF217* (aa 1–283), 2. aa 35–211, 3. aa 5–87, 4. aa 35–164, 5. aa 159–283, 6. aa 159–211, 7. aa 194–283, 8. aa 36–211) in frame into the pGBKT7 vector (Clontech, Heidelberg, Germany) to be expressed as GAL4-DBD fusion proteins. A commercially available HeLa S3 cDNA library cloned into the pGAD-GH vector to give rise to proteins as GAL4-AD fusions (Clontech) was used as prey library. To map the *RNF217* interaction with HAX1, full-length HAX1 was cloned into a modified pGADT7 vector. For intracellular localization experiments, *RNF217* and *HAX1* were cloned into the vectors pECFP and cEYFP, respectively (Clontech).

**Characterization of the *RNF217* gene.** The human *RNF217* gene was mapped from the UniGene database clone IMAcGp998E064109Q2 (reference AA992964). Sequence homology was assessed by BLAST and protein domains were identified using PROSITE pattern search.

**Human multiple tissue Northern blot.** A human multiple tissue northern blot (Clontech) was hybridized with a radioactively labeled (Megaprime kit, Amersham Pharmacia Biotech Freiburg, Germany) 748 bp *RNF217* cDNA probe, PCR amplified from mouse testis cDNA using the primers 5'-CTACCTCGAGAGATGAAGGTAC-AACTTGGCC-3' and 5'-CATACTGCAGTGTACCAGTGCATACCTGTCCG-3'. The blot was subjected to autoradiography, stripped and reprobed for  $\beta$ -actin.

### Expression of *RNF217* in human B cells/B cell leukemia cell lines and human leukemia patient bone marrow samples.

B cell developmental stages were flow sorted from bone marrow (BM) and peripheral blood (PB) (pre-B: BM, CD19<sup>+</sup>VpreB<sup>+</sup>; B1: PB, CD19<sup>+</sup>CD5<sup>+</sup>; naïve: PB, CD19<sup>+</sup>CD27<sup>+</sup>; memory: PB, CD19<sup>+</sup>CD27<sup>+</sup>; plasma cells: PB, CD19<sup>+</sup>CD38<sup>high</sup>CD138<sup>+</sup>) on an Epics Elite cell sorter (Beckman Coulter, Krefeld, Germany) into RNA later solution (Ambion, Austin, TX, USA).

Total RNA was extracted using QiaShredder columns and the RNeasy Mini Kit (both from Qiagen, Hilden, Germany). RNA was reverse transcribed using Superscript reverse transcriptase (Invitrogen, Darmstadt, Germany) and amplified with primers as follows: For human B cell leukemia cell lines and primary human bone marrow/leukemia samples: *RNF217* 5'-AGAGGAATGCCGAGAAGTGCC-3' and 5'-ACTGAGGTTTGTATGTGTGGTCTCC-3', *TBP* 5'-GCACAGGAG-CCAAGAGTGAA-3' and 5'-TCACAGCTCCCACCATTGTT-3'. For the human B cell developmental stages: *RNF217* 5'-GAGTGCTCAAAGTCTACCTG-3' and 5'-CATACTGCAGTGTACCAGTGCATACCTGTCCG-3', *GAPDH* 5'-GCACCA-CCAAGTCTTAGCACC-3' and 5'-GTCTGAGTGTGGCAGGGACTC-3'. For quantitative RT-PCR, cDNA derived from primary human leukemia samples was amplified with the primers *RNF217* 5'-TCCCAGAGAGACCTCATTTAAGGA-3' and 5'-CCCTAGTGCCAATCCCAAAA-3' together with the TaqMan (FAM/BHQ-1) probe 5'-CGAGGGTCAGTCTGTGCTGGAAAATTATTCAT-3'. The human  $\beta$ -actin endogenous control (VIC/TAMRA probe) (Life Technologies, Darmstadt, Germany) was used for normalization. Relative *RNF217* expression levels were determined using the  $\Delta\Delta C_T$  method.

**Yeast two-hybrid screen and mapping of *RNF217*-HAX1 interaction.** The yeast strain AH109 (Clontech) was co-transformed with the pGAD-GH prey plasmid containing the human cDNA HeLa S3 library and the pGBKT7-*RNF217* bait plasmid by lithium acetate transformation. Clones harboring interacting bait/prey proteins grew in the absence of tryptophan, leucine, histidine, and adenine, and showed X-gal activity. Positive clones were sequenced and annotated. For the mapping of the interaction between *RNF217* and HAX1, *RNF217* deletion mutants were cloned into the pGBKT7 bait plasmid and full-length HAX1 into the pGADT7 plasmid. Both plasmids were used to cotransform AH109 yeast cells.

**Transfection of adherent cells.** Cells were transiently transfected using cationic polymers (RothFect, Carl Roth, Darmstadt, Germany or PolyFect, Qiagen). For fluorescence microscopy, NIH3T3 cells were grown on cover slips for 12–24 h after transfection, fixed with formaldehyde, mounted on glass slides, and analyzed using an inverted fluorescence microscope (Axiovert 200 M, Carl Zeiss, Goettingen, Germany).

**In vitro co-immunoprecipitation of *RNF217* and HAX1.** Radioactively labeled [<sup>35</sup>S]-proteins were produced using the TNT-reticulocyte-lysate system (Promega, Mannheim, Germany). *RNF217* was expressed from the pGBKT7 vector to give rise to a HA-tagged protein, HAX1 was expressed from the pGADT7 vector to give rise to a myc-tagged protein. The *in vitro* translated proteins were mixed 1:1 and immunoprecipitated with an anti-HA (*RNF217*) or an anti-myc antibody (HAX1) together with protein A beads (Clontech). Proteins were separated by SDS-PAGE, the gel was fixed and incubated with fluorographic amplification reagent (Amersham) before being exposed to an X-ray film (Kodak, Stuttgart, Germany).

pCFP-*RNF217* and pYFP-HAX1 were co-transfected into HEK293T cells and the cells were lysed 24 h later. HAX1 was immunoprecipitated with a mouse anti-HAX1 antibody (Clontech) or control polyclonal mouse IgG (Santa Cruz, Heidelberg, Germany) and protein G-agarose beads (Roche, Mannheim, Germany). Proteins were separated by SDS-PAGE, blotted on nitrocellulose membranes (BioRad, Munich, Germany) by semi-dry blotting (BioRad), and CFP-*RNF217* was detected using an anti-GFP antibody (Molecular Probes, Darmstadt, Germany) with an HRP-conjugated secondary anti-mouse antibody (Santa Cruz) and enhanced chemiluminescence detection (Amersham).

**Statistics.** For the statistical analysis of qRT-PCR data (Figure 4c), normality for all groups was tested for by the Shapiro-Wilk test. ALL and AML samples were identified to be not normally distributed. Therefore, all groups were compared using the non-parametric Mann-Whitney U test. Differences with a P-value below 0.01 were seen as statistically highly significant and marked \*\*.

1. Rowley, J. D. The role of chromosome translocations in leukemogenesis. *Semin. Hematol.* **36**, 59–72 (1999).
2. Bohlander, S. K. Fusion genes in leukemia: An emerging network. *Cytogenet. Cell Genet.* **91**, 52–56 (2000).
3. Martens, J. H. A. & Stunnenberg, H. G. The molecular signature of oncogenic proteins in acute myeloid leukemia. *FEBS Lett.* **584**, 2662–2669 (2010).





4. Rabbitts, T. H. Chromosomal translocations in human cancer. *Nature* **372**, 143–149 (1994).
5. Alcalay, M. *et al.* Acute myeloid leukemia fusion proteins deregulate genes involved in stem cell maintenance and DNA repair. *J. Clin. Invest.* **112**, 1751–1761 (2003).
6. Biswas, D. *et al.* Function of leukemogenic mixed lineage leukemia 1 (MLL) fusion proteins through distinct partner protein complexes. *Proc. Natl. Acad. Sci. U. S. A.* **108**, 15751–15756 (2011).
7. Golub, T. R., Barker, G. F., Lovett, M. & Gilliland, D. G. Fusion of PDGF receptor beta to a novel ets-like gene, tel, in chronic myelomonocytic leukemia with t(5;12) chromosomal translocation. *Cell* **77**, 307–316 (1994).
8. De Braekeleer, E. *et al.* ETV6 fusion genes in hematological malignancies: A review. *Leuk. Res.* **36**, 945–961 (2012).
9. Bohlander, S. K. ETV6: A versatile player in leukemogenesis. *Semin. Cancer Biol.* **15**, 162–174 (2005).
10. Suto, Y., Sato, Y., Smith, S. D., Rowley, J. D. & Bohlander, S. K. A t(6;12)(q23;p13) results in the fusion of ETV6 to a novel gene, STL, in a b-cell ALL cell line. *Genes Chromosomes Cancer* **18**, 254–268 (1997).
11. Zhang, L. Q. *et al.* Establishment of cell lines from b-cell precursor acute lymphoblastic leukemia. *Leukemia* **7**, 1865–1874 (1993).
12. Kobayashi, H. *et al.* Fluorescence in situ hybridization mapping of translocations and deletions involving the short arm of human chromosome 12 in malignant hematologic diseases. *Blood* **84**, 3473–3482 (1994).
13. Hayashi, Y. *et al.* Abnormalities of the long arm of chromosome 6 in childhood acute lymphoblastic leukemia. *Blood* **76**, 1626–1630 (1990).
14. Bouska, A. *et al.* Genome-wide copy number analyses reveal genomic abnormalities involved in transformation of follicular lymphoma. *Blood* **123**, 1681–1690 (2014).
15. Rowley, J. D. Recurring chromosome abnormalities in leukemia and lymphoma. *Semin. Hematol.* **27**, 122–136 (1990).
16. Jadayel, D. M. *et al.* Potential role for concurrent abnormalities of the cyclin D1, p16cdkn2 and p15cdkn2b genes in certain B cell non-hodgkin's lymphomas. Functional studies in a cell line (granta 519). *Leukemia* **11**, 64–72 (1997).
17. Greil, J. *et al.* The acute lymphoblastic leukaemia cell line SEM with t(4;11) chromosomal rearrangement is biphenotypic and responsive to interleukin-7. *Br. J. Haematol.* **86**, 275–283 (1994).
18. Huang, H. *et al.* TEL1 plays an essential oncogenic role in MLL-rearranged leukemia. *Proc. Natl. Acad. Sci. U. S. A.* **110**, 11994–11999 (2013).
19. Mulaw, M. A. *et al.* CALM/AF10-positive leukemias show upregulation of genes involved in chromatin assembly and DNA repair processes and of genes adjacent to the breakpoint at 10p12. *Leukemia* **26**, 1012–1019 (2012).
20. Lin, Y.-H. *et al.* Global reduction of the epigenetic H3K79 methylation mark and increased chromosomal instability in CALM-AF10-positive leukemias. *Blood* **114**, 651–658 (2009).
21. Greif, P. A., Tizazu, B., Krause, A., Kremmer, E. & Bohlander, S. K. The leukemogenic CALM/AF10 fusion protein alters the subcellular localization of the lymphoid regulator ikaros. *Oncogene* **27**, 2886–2896 (2008).
22. Budhidarmo, R., Nakatani, Y. & Day, C. L. RINGs hold the key to ubiquitin transfer. *Trends Biochem. Sci.* **37**, 58–65 (2012).
23. Xu, G. W. *et al.* The ubiquitin-activating enzyme E1 as a therapeutic target for the treatment of leukemia and multiple myeloma. *Blood* **115**, 2251–2259 (2010).
24. Wang, E. *et al.* Histone H2B ubiquitin ligase RNF20 is required for mll-rearranged leukemia. *Proc. Natl. Acad. Sci. U. S. A.* **110**, 3901–3906 (2013).
25. Guan, D., Factor, D., Liu, Y., Wang, Z. & Kao, H.-Y. The epigenetic regulator UHRF1 promotes ubiquitination-mediated degradation of the tumor-suppressor protein promyelocytic leukemia protein. *Oncogene* **32**, 3819–3828 (2013).
26. Reavie, L. *et al.* Regulation of c-myc ubiquitination controls chronic myelogenous leukemia initiation and progression. *Cancer Cell* **23**, 362–375 (2013).
27. Niewerth, D., Dingjan, I., Cloos, J., Jansen, G. & Kaspers, G. Proteasome inhibitors in acute leukemia. *Expert Rev. Anticancer Ther.* **13**, 327–337 (2013).
28. Masetti, R., Kleinschmidt, K., Biagi, C. & Pession, A. Emerging targeted therapies for pediatric acute myeloid leukemia. *Recent. Pat. Anticancer Drug Discov.* **6**, 354–366 (2011).
29. Colado, E. *et al.* The effect of the proteasome inhibitor bortezomib on acute myeloid leukemia cells and drug resistance associated with the CD34+ immature phenotype. *Haematologica* **93**, 57–66 (2008).
30. Tagawa, H. *et al.* Molecular cytogenetic analysis of the breakpoint region at 6q21-22 in t-cell lymphoma/leukemia cell lines. *Genes Chromosomes Cancer* **34**, 175–185 (2002).
31. Gorbea, C. *et al.* A protein interaction network for ecm29 links the 26 S proteasome to molecular motors and endosomal components. *J. Biol. Chem.* **285**, 31616–31633 (2010).
32. Suzuki, Y. *et al.* HAX-1, a novel intracellular protein, localized on mitochondria, directly associates with HS1, a substrate of src family tyrosine kinases. *J. Immunol.* **158**, 2736–2744 (1997).
33. Klein, C. *et al.* HAX1 deficiency causes autosomal recessive severe congenital neutropenia (Kostmann disease). *Nat. Genet.* **39**, 86–92 (2007).
34. Li, B. *et al.* Hax-1 is rapidly degraded by the proteasome dependent on its PEST sequence. *BMC Cell Biol.* **13**, 20 (2012).
35. Cilenti, L. *et al.* Regulation of HAX-1 anti-apoptotic protein by omi/htra2 protease during cell death. *J. Biol. Chem.* **279**, 50295–50301 (2004).
36. Lee, A. Y. *et al.* HS 1-associated protein X-1 is cleaved by caspase-3 during apoptosis. *Mol. Cells* **25**, 86–90 (2008).
37. Han, J. *et al.* Deregulation of mitochondrial membrane potential by mitochondrial insertion of granzyme B and direct hax-1 cleavage. *J. Biol. Chem.* **285**, 22461–22472 (2010).
38. Chao, J.-R. *et al.* Hax1-mediated processing of htra2 by parl allows survival of lymphocytes and neurons. *Nature* **452**, 98–102 (2008).
39. Kang, Y. J. *et al.* Molecular interaction between HAX-1 and XIAP inhibits apoptosis. *Biochem. Biophys. Res. Commun.* **393**, 794–799 (2010).
40. Han, Y. *et al.* Overexpression of HAX-1 protects cardiac myocytes from apoptosis through caspase-9 inhibition. *Circ. Res.* **99**, 415–423 (2006).
41. Sun, S.-J., Feng, L., Zhao, G.-Q. & Dong, Z.-M. HAX-1 promotes the chemoresistance, invasion, and tumorigenicity of esophageal squamous carcinoma cells. *Dig. Dis. Sci.* **57**, 1838–1846 (2012).
42. Kwiecinska, A. *et al.* HAX-1 expression in human B lymphoma. *Leukemia* **25**, 868–872 (2011).
43. Peckl-Schmid, D. *et al.* HAX1 deficiency: Impact on lymphopoiesis and B-cell development. *Eur. J. Immunol.* **40**, 3161–3172 (2010).
44. Skokowa, J. *et al.* Interactions among HCLS1, HAX1 and LEF-1 proteins are essential for g-csf-triggered granulopoiesis. *Nat. Med.* **18**, 1550–1559 (2012).
45. Vandenberghe, P. & Beel, K. Severe congenital neutropenia, a genetically heterogeneous disease group with an increased risk of AML/MDS. *Pediatr. Rep.* **3 Suppl2**, e9 (2011).
46. Pelechano, V. & Steinmetz, L. M. Gene regulation by antisense transcription. *Nature Reviews Genetics* **14**, 880–893 (2013).
47. Guil, S. & Esteller, M. Cis-acting noncoding rRNAs: Friends and foes. *Nat. Struct. Mol. Biol.* **19**, 1068–1075 (2012).
48. Yang, P. K. & Kuroda, M. I. Noncoding rnas and intranuclear positioning in monoallelic gene expression. *Cell* **128**, 777–786 (2007).
49. Pontier, D. B. & Gribnau, J. Xist regulation and function explored. *Hum. Genet.* **130**, 223–236 (2011).
50. Zhang, H. *et al.* Long noncoding rna-mediated intrachromosomal interactions promote imprinting at the kcnq1 locus. *J. Cell Biol.* **204**, 61–75 (2014).
51. Lyle, R. *et al.* The imprinted antisense RNA at the igf2r locus overlaps but does not imprint mas1. *Nat. Genet.* **25**, 19–21 (2000).
52. Nagano, T. *et al.* The air noncoding RNA epigenetically silences transcription by targeting g9a to chromatin. *Science* **322**, 1717–1720 (2008).
53. Azzi, S., Abi Habib, W. & Netchine, I. Beckwith-Wiedemann and Russell-Silver syndromes: From new molecular insights to the comprehension of imprinting regulation. *Curr. Opin. Endocrinol. Diabetes Obes.* **21**, 30–38 (2014).
54. Vu, T. H., Chuyen, N. V., Li, T. & Hoffman, A. R. Loss of imprinting of IGF2 sense and antisense transcripts in wilms' tumor. *Cancer Res.* **63**, 1900–1905 (2003).
55. Pang, K. C. *et al.* Genome-wide identification of long noncoding rnas in CD8+ T cells. *J. Immunol.* **182**, 7738–7748 (2009).
56. Peeters, P. *et al.* Fusion of ETV6 to MDS1/EVI1 as a result of t(3; 12)(q26; p13) in myeloproliferative disorders. *Cancer Res.* **57**, 564–569 (1997).
57. Cools, J. *et al.* Evidence for position effects as a variant etv6-mediated leukemogenic mechanism in myeloid leukemias with at t(4;12)(q11-q12;p13) or t(5; 12)(q31; p13). *Blood* **99**, 1776–1784 (2002).
58. Jalali, G. R. *et al.* Disruption of ETV6 in intron 2 results in upregulatory and insertional events in childhood acute lymphoblastic leukaemia. *Leukemia* **22**, 114–123 (2008).
59. Rawat, V. P. S. *et al.* Ectopic expression of the homeobox gene Cdx2 is the transforming event in a mouse model of t(12; 13)(p13; q12) acute myeloid leukemia. *Proc. Natl. Acad. Sci. U. S. A.* **101**, 817–822 (2004).

## Acknowledgments

This work was supported by the Deutsche Forschungsgemeinschaft (DFG grant SFB 684 A6). L.F.K. was supported by a fellowship of the Deutsche José Carreras Leukämienstiftung. S.K.B. and M.C. are support by Leukaemia & Blood Cancer New Zealand and the family of Marijanna Kumerich.

## Author contributions

L.M.F.K. and S.K.B. conceived and designed this study. L.M.F.K., A.S.J., A.K., and J.M. performed experiments and analysed data. M.C. analysed data. S.K.B. supervised the study. L.M.F.K., M.C., M.M. and S.K.B. wrote the manuscript.

## Additional information

Supplementary information accompanies this paper at <http://www.nature.com/scientificreports>

**Competing financial interests:** The authors declare no competing financial interests.

**How to cite this article:** Fontanari Krause, L.M. *et al.* Identification and characterization of *OSTL (RNF217)* encoding a RING-IBR-RING protein adjacent to a translocation breakpoint involving *ETV6* in childhood ALL. *Sci. Rep.* **4**, 6565; DOI:10.1038/srep06565 (2014).



This work is licensed under a Creative Commons Attribution-NonCommercial-ShareAlike 4.0 International License. The images or other third party material in this article are included in the article's Creative Commons license, unless indicated otherwise in the credit line; if the material is not included under the Creative

Commons license, users will need to obtain permission from the license holder in order to reproduce the material. To view a copy of this license, visit <http://creativecommons.org/licenses/by-nc-sa/4.0/>